Computer Simulation of Selective Aggregation in Binary Colloids

F. Pierce,* A. Chakrabarti, D. Fry,† and C. M. Sorensen

Kansas State University, 316 Cardwell Hall, Manhattan, Kansas 66506

Received September 3, 2003. In Final Form: November 14, 2003

The morphology of clusters formed by selective aggregation of binary colloids is studied in a two-dimensional Monte Carlo simulation for a large range of number fractions (200:1, 100:1, 10:1, 2:1). We find remarkable similarity in morphology to those observed in experiments, from the formation of closed "micelles" to large branched clusters. Quantitative studies of the fractal dimension, kinetics, and cluster size distribution are also carried out and compared with diffusion-limited cluster aggregation and reaction-limited cluster aggregation models.

Introduction

The process of aggregation is integral to the formation of fractal aggregates in colloids and aerosols.[1,2] Such aggregates are common in nature and important for our technology with many applications in biological systems, the medical industry, paints and coatings, and numerous foods. Limiting nonequilibrium models, such as the diffusion-limited cluster aggregation (DLCA) and reaction-limited cluster aggregation model (RLCA), exist and have been successful in describing aggregation in aerosols and colloids.[3] Much recent work, however, has focused on tailoring the interaction between colloidal particles so that a greater control over the self-assembly of these particles (and hence their material properties) can be obtained. This can be achieved in several ways. One typical way to vary the interaction between charged colloidal particles is to add salt or surfactant solution of different molarities.[4] Another way to modify the interaction between colloidal particles is to induce a depletion interaction[5−7] by the addition of a nonadsorbing polymer (or a different-sized colloid[8]). The strength and range of the interaction can be controlled in this case by changing the concentration and the length of the polymer chain. Depletion colloids are known to exhibit transient gel formation, reversible aggregation, and eventual crystallization.[9] A different route has recently been taken by Hiddessen et al.[10] to control the assembly of *binary* colloidal particles. They introduce specific biomolecular cross-linking among smaller and larger diameter particles by coating these particles with complementary biological proteins. These proteins behave as specific lock-and-key molecules and mediate adhesion only between two different-sized colloidal particles but not among particles of the same size. A progressive series of structures from micelles to fractal-like elongated chains have been observed in the experiment as the ratio of the number of small to big particles was changed.

For a quantitative understanding of the structures formed in the above-mentioned binary colloids, we have carried out a variation of the off-lattice DLCA model by considering a bidisperse system where a *selective* aggregation can occur only when two different-sized particles come into contact. Our current study is totally different from past work in this context, where either (i) a nonselective aggregation among polydisperse particles was considered[11] or (ii) a selective aggregation was studied among particles of the *same* size.[12] None of these previous studies seem to yield the variety of cluster morphologies observed in the Hiddessen et al. experiment. In contrast, our simulations reproduce much of the experimentally observed structures as a function of the ratio of the number of small to big particles. We also study quantitative measures of the aggregation process such as the kinetics of aggregation and cluster size distribution and compare our results to those for monodisperse off-lattice DLCA (and to some extent to RLCA) aggregation.

Model and Numerical Procedure

In the model bidisperse system, we consider $N_s = 20\,000$ small particles of radius $r_s = 1$ unit and a variable number (N_L) of large particles of radius $r_L = 5$ units. This closely resembles the particle sizes used in the experimental study of Hiddessen et al. who have used spheres of size 0.94 and 5.5 μm. Values of N_L are chosen to be 100, 200, 2000, and 10 000 for the number ratio $n_R = N_s/N_L$ to be 200, 100, 10, and 2, respectively. We chose these number fractions closely following the ones by Hiddessen et al. for a direct comparison of simulated cluster morphologies with experimental observations. Both the small and large particles were randomly placed in a *two-dimensional* simulation box of linear size L (in units of the *diameter* of the small particles) with a desired total area fraction of 10%.

Periodic boundary conditions were used in the simulation, and a link-cell algorithm[13,14] was employed to significantly reduce computation time.

† Present address: Polymers Division, National Institute of Standards and Technology, Gaithersburg, MD 20899.

(1) Russel, W. B.; Saville, D. A.; Schowalter, W. R. *Colloidal dispersions*; Cambridge University Press: Cambridge, 1989.

(2) Friedlander, S. K. *Smoke, Dust and Haze*; Oxford University Press: Oxford, 2000.

(3) Meakin, P. A historical introduction to computer models for fractal aggregates. *J. Sol.-Gel Sci. Technol.* **1999**, *15*, 97−117.

(4) Hunter, R. *Foundations of colloid science*; Clarendon Press: Oxford, 1987.

(5) Asakura, S.; Oosawa, F. On interaction between two bodies immersed in a solution of macromolecules. *J. Chem. Phys.* **1954**, *22*, 1255−1256.

(6) Vrij, A. Polymers at interfaces and the interaction in colloidal dispersions. *Pure Appl. Chem.* **1976**, *48*, 471−473.

(7) Verma, R.; Crocker, J. C.; Lubensky, T. C.; Yodh, A. G. Attractions between hard colloidal spheres in semiflexible polymer solutions. *Macromolecules* **2000**, *33*, 177−186.

(8) Hobbie, E. K. Metastability and Depletion-Driven Aggregation. *Phys. Rev. Lett.* **1998**, *81*, 3996−3999.

(9) Anderson, V. J.; Lekkerkerker, H. N. W. Insights into phase transition kinetics from colloid science. *Nature* **2002**, *416*, 811−815.

(10) Hiddessen, A.; Rodgers, S.; Weitz, D.; Hammer, D. Assembly of Binary Colloidal Structures via Specific Biological Adhesion. *Langmuir* **2000**, *16*, 9744−9753.

(11) Bushell, G.; Amal, R. Fractal Aggregates of Polydisperse Particles. *J. Colloid Interface Sci.* **1998**, *205*, 459−469.

(12) Meakin, P.; Miyazima, S. Reaction Limited Aggregation with Two Species of Monomers. *J. Phys. Soc. Jpn.* **1988**, *57*, 4439−4449.

10.1021/la0356452 CCC: $27.50
Published on Web 02/11/2004

We begin by randomly picking, with probability N_c^{-1}, a cluster of size N (number of monomers per cluster), where N_c is the number of clusters at time t. Invoking Stokes−Einstein type diffusion, once a cluster is picked, it is moved with a probability $D_0 = R_g^{-1}$ where R_g is the cluster's radius of gyration. The distance moved is one small monomer diameter d_s. Each time a cluster is picked, the time, measured in Monte Carlo steps per cluster, is incremented by N_c^{-1}.

When a collision between two clusters occurred, a test was made to see whether the contact particles in the two clusters were of the same or different size. If the particles were of different sizes, the clusters were joined into one cluster and the aggregation process was allowed to continue. If the particles were of the same size, no joining occurred, and the clusters were permitted to diffuse away from one another. In each case, the motion of clusters is adjusted in order to correct for any overlap between particles. The cluster number and size distribution along with its moments, free volume, and radius of gyration are monitored throughout the simulation. Results are averaged over 10 runs.

Besides the simulation being in two dimensions, the area fraction of 10% considered in the simulation is much larger than the volume fraction (typically 10^{-4}−10^{-3}) used in the experimental study of Hiddessen et al. Our choice of an area fraction of 10% had much to do with the prohibitively long computer time taken for the observance of aggregation in a very dilute system. Still, even in our relatively dense case, the simulation shows remarkable qualitative similarity to the experimental results. In addition, we present quantitative measurements for

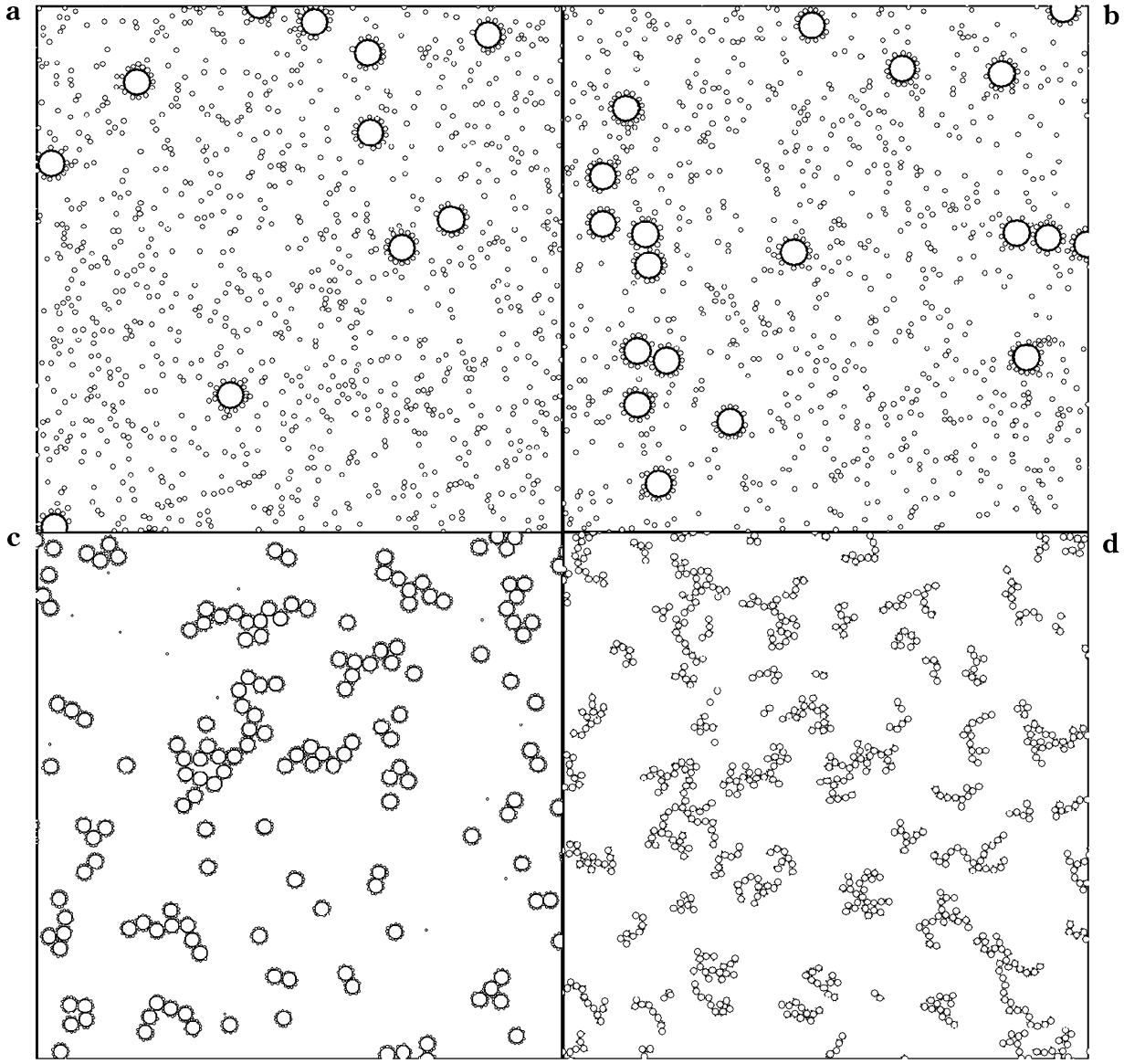

Figure 1. Panel a (top left): Late time snapshots of 20 000 small particles with 100 large particles (number fraction 200:1). Notice the predominance of clusters containing only 1 large particle. The box dimensions are 420 × 420 in units of the *diameter* of the small particles. The current view is set to a 100 × 100 section. The apparent "clusters" of small particles alone are not actually clusters. The simulation allows small particles to touch each other but then diffuse away in later steps. Panel b (top right): 20 000 small particles with 200 large particles (number fraction 100:1). In this situation, most clusters contain only a few large particles. The box dimensions are 440 × 440. The current view is set to 100 × 100. Panel c (bottom left): 20 000 small particles with 2000 large particles (number fraction 10:1). Notice the larger clusters containing several large particles as well as the almost complete absence of monomers. The box dimensions are 740 × 740. The current view is set to 200 × 200. Panel d (bottom right): 20 000 small particles with 10 000 large particles (number fraction 2:1) at $t = 12\,650$. Now we see many larger clusters containing several large particles and the complete absence of monomers. The box dimensions are 1450 × 1450. The current view is set to 400 × 400.

fractal dimension, aggregation kinetics, and cluster size distribution. Finally, some differences between this system and the monodisperse 2D DLCA case are discussed.

Results

In Figure 1a−d, we display the morphology of clusters obtained for various values of the number ratio n_R. For $n_R = 200$, we observe in Figure 1a that the system quickly falls into a nonaggregating state where large particles are completely coated by small particles and no further aggregation takes place. Clusters in this case are either single small particles or "micelles" with one large particle completely encased in small particles. This compares extremely well with the experimental situation for a comparable value of n_R. One must be careful not to view the groupings of small particles together in this figure as clusters. Our simulation allows same-size particles to come in contact but not to join into a cluster when they touch.

When n_R is decreased to 100 (Figure 1b), clusters involving more than a single large particle start forming. Predominantly the clusters involve only two large particles. Again, this is very similar to what was observed in the experiment. Larger clusters (up to 5 or more large particles) are seen when n_R is further decreased to 10 (Figure 1c). The "cloud" of small particles seen in Figure 1a,b has now been almost completely swept away by aggregation with large particles; almost all of the small particles are now involved in multiple-particle clusters. The experiment also seemed to indicate this removal of stray small particles from the system.

For $n_R = 2$, fractal clusters are readily formed as shown in Figure 1d. To quantify the fractal nature of these clusters, we have run the simulation for a much longer time ($t = 1\,997\,850$) than shown in Figure 1d ($t = 12\,650$). Such a late time ($t = 1\,997\,850$) configuration (Figure 2a) shows an ensemble of clusters quite similar to what has been observed in previous studies of 2D DLCA or RLCA models. The smaller particles cannot be seen in Figure 2a, but their presence becomes apparent when we zoom into one of the clusters (see Figure 2b).

After being able to reproduce various cluster morphologies seen in the experiment, we now focus on the case for $n_R = 2$ and carry out a quantitative analysis of our results. First, we compute the fractal dimension of the ensemble of clusters in this case by plotting the mass M of a cluster versus radius of gyration R_g in an ensemble of clusters (Figure 3a). The fractal dimension of the clusters, D_f, is then determined from the slope of such a log−log graph. Figure 3b is a graph of the evolution of D_f with time averaged over 10 runs of the simulation. The value of D_f ranges from about 1.40 at $t = 15\,300$ to 1.54 at $t = 382\,700$. For early times, the value of the fractal dimension is similar to the accepted value for 2D DLCA.[15] This is remarkable given the selective nature of the aggregation process here. Although not all cluster collisions result in the formation of a new cluster, a sufficiently large number of these collisions produce aggregation at earlier times, presumably due to the availability of a large number of small particles at earlier times. In addition, the larger particles can be decorated by more than one small particle, and this provides a considerably larger probability of aggregation than in past studies of selective aggregation with *same*-sized particles,[12] where the system behaves like a RLCA system over the entire evolution process. At later times, there are fewer small particles present in our system and now, most collisions do not lead to the formation of aggregates. It is possible then that the binary colloid system may cross over from a DLCA morphology at early times to an RLCA morphology at late times. The signature of this is present in the fractal dimension of the clusters which slowly increases from the 2D DLCA value of 1.4 and approaches the 2D RLCA[15] value of ∼1.55.

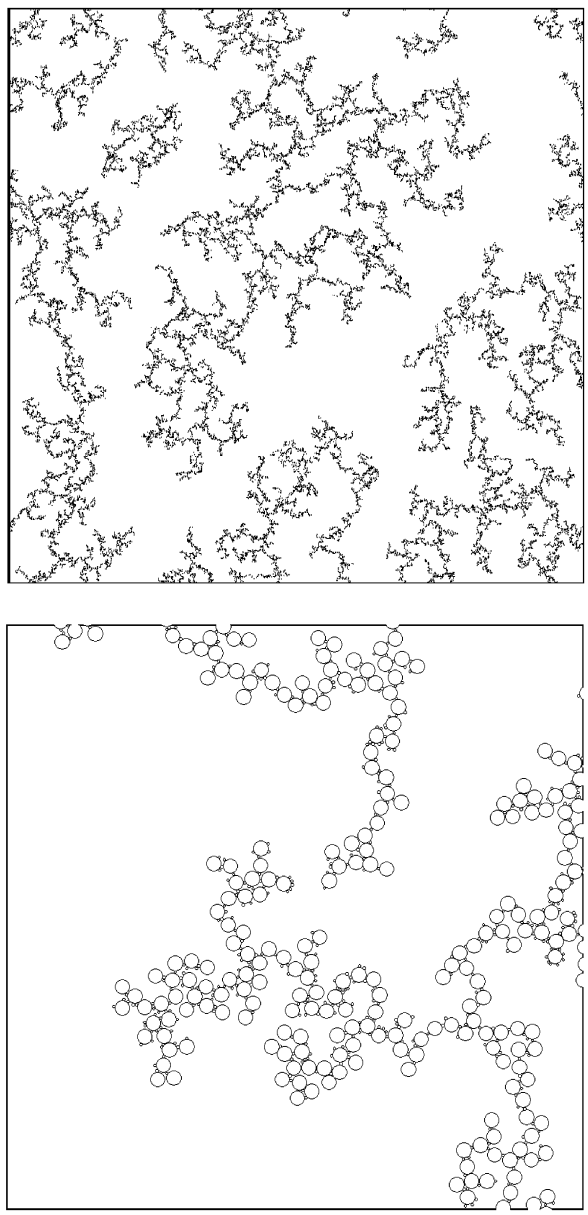

Figure 2. Panel a: 20 000 small particles with 10 000 large particles (number fraction 2:1) at $t = 1\,997\,850$. We observe very large branched clusters containing hundreds of large particles as well as many small particles which at this scale are nearly invisible. The small particles act like glue for the large particles to stick together in clusters. The box dimensions are 1450 × 1450 as is the current view. Panel b: The same simulation as panel a, but focused into a current view of 250 × 250. At this level of focus, we can see the small particles that were invisible in panel a.

Results for the kinetics of aggregation are presented in Figure 4a, where we show a log−log plot of $N_c^{-1}(t) - N_c^{-1}(0)$ versus time t. The slope of this graph yields the kinetic exponent[16] z. The value obtained for z in this case is $z = 0.74 \pm 0.04$ in the intermediate time as shown by the straight line in the graph. A scaling argument[17,18] yields $z = 0.59$ in the dilute limit of the 2D DLCA model. It is known, however, that the value of z increases from this dilute limit value as the system becomes dense due to cluster crowding.[13,14] Indeed, for intermediate times, the scaling argument[18] yields $z = 0.67$ for the 2D DLCA model. Even larger values of the kinetic exponent have

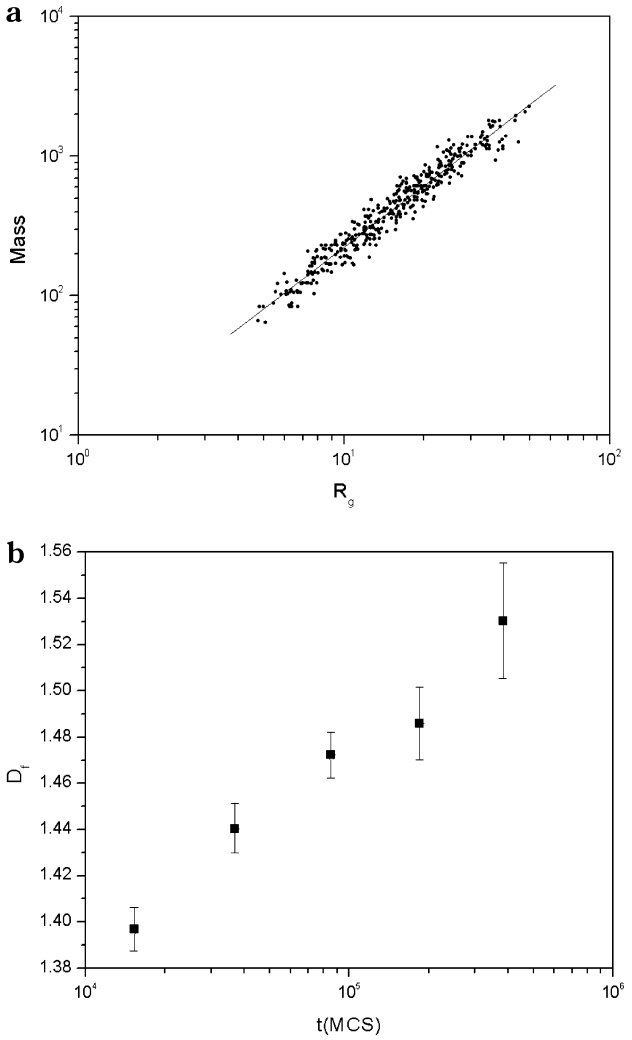

Figure 3. Panel a: Fractal dimension of clusters formed with number fraction 2:1 at time $t = 38\,276$ with $N_c = 414$. The value obtained from the slope of a linear fit to $\log(M)$ vs $\log(R_g)$ is 1.46. Panel b: Fractal dimension vs time in Monte Carlo steps of clusters formed with number fraction 2:1 for times ranging from 10 000 to 1 million. The fractal dimension varies continuously from nearly 1.4 (similar to 2D DLCA) to a value of 1.54 consistent with 2D RLCA ($D_f = 1.55$) as the time evolves. All values were derived from a sample of 10 runs. Error bars represent standard errors of values. The large standard errors at late times are due to a relatively smaller number of clusters in the system.

been observed at intermediate times in simulations of 2D DLCA for larger area fractions.[13] There is also a hint of an increase of the kinetic exponent at later times in Figure 4a due to cluster crowding.

In contrast, one might expect that for larger values of n_R (n_R = 200, 100, or 10), the system would enter a nonaggregating state at late times when further aggregation becomes impossible. In the case of number fraction $n_R = 200$ or 100, this is obvious, since each large particle can be surrounded only by a finite number of small particles. Once all of the large particles are completely surrounded, further aggregation halts. A corresponding slowdown in kinetics is also observed for $n_R = 10$ (Figure 4b). Here, at intermediate times, the kinetic exponent is $z = 0.74 \pm 0.04$ as in the case of $n_R = 2$, but a distinct slowdown in the kinetics of aggregation is observed at late times. For $n_R = 2$, such a slowdown is difficult to observe in the simulations unless one considers late time studies in a very large system (with a much larger number of particles but yet with a much smaller volume fraction).

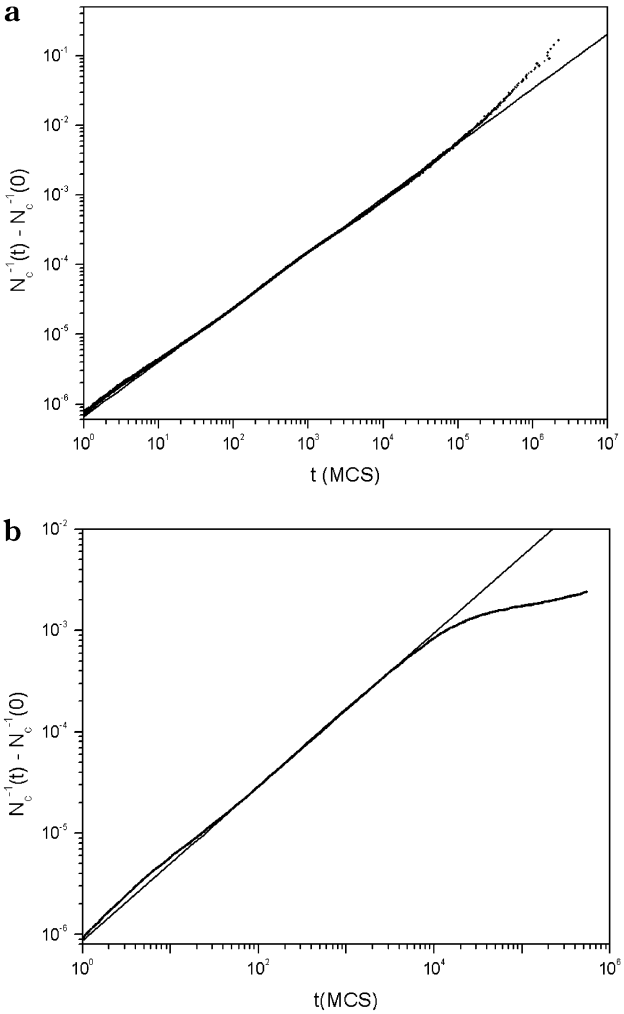

Figure 4. Panel a: Graph of $N_c^{-1}(t) - N_c^{-1}(0)$ vs t for $n_R = 2$. The straight line fit at the intermediate times yields the kinetic exponent $z = 0.74 \pm 0.05$. Panel b: Same as in panel a except for $n_R = 10$. The straight line fit at the intermediate times yields the kinetic exponent $z = 0.74 \pm 0.05$. Note the slowdown in the kinetics at late times.

The similarity between the current simulation of binary colloids with $n_R = 2$ and 2D DLCA is further explored by computing cluster size distributions. In Figure 5a, we show the cluster size distribution at various times. The common tangent line is included as well, yielding a slope of ca. −2.05, in good agreement with theoretical predictions.[19] In Figure 5b, we plot the scaled (and normalized such that the maximum value of the function is unity) cluster size distribution. This graph demonstrates that scaling works well for the current simulations. We define M_p to

(13) Fry, D. Aggregation in Dense Particulate Systems. Ph.D. Thesis, Kansas State University, Manhattan, KS, 2003.
(14) Fry, D.; Sintes, T.; Chakrabarti, A.; Sorensen, C. M. Enhanced kinetics and free-volume universality in dense aggregating systems. *Phys. Rev. Lett.* **2002**, *89*, 148301 (1-4).
(15) Family, F.; Meakin, P.; Vicsek, T. Cluster size distribution in chemically controlled cluster−cluster aggregation. *J. Chem. Phys.* **1985**, *83*, 4144−4150.
(16) van Dongen, P. G. J.; Ernst, M. H. Dynamic scaling in the kinetics of clustering. *Phys. Rev. Lett.* **1985**, *54*, 1396−1399.
(17) Kolb, M. Unified description of static and dynamic scaling for kinetic cluster formation. *Phys. Rev. Lett.* **1984**, *53*, 1653−1656.
(18) Chakrabarti, A.; Fry, D.; Sorensen, C. M. Molecular dynamics simulation of the transition from dispersed to solid phase. Preprint 2003.
(19) Meakin, P.; Vicsek, T.; Family, F. Dynamic cluster-size distribution in cluster−cluster aggregation: Effects of cluster diffusivity. *Phys. Rev. B* **1985**, *31*, 564−569.

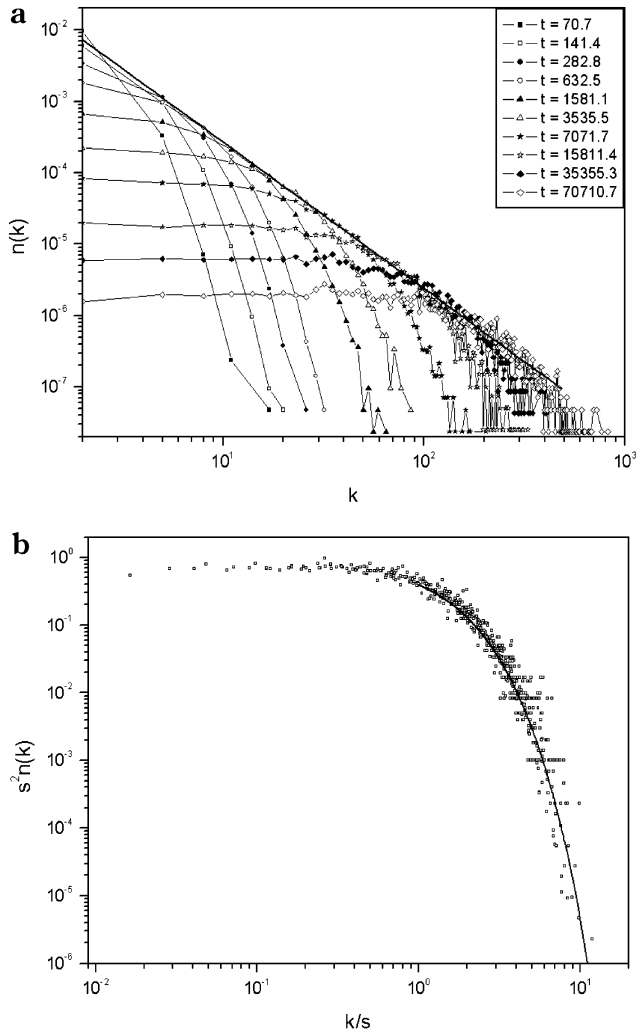

Figure 5. Panel a: Cluster size distributions for various times during the simulation along with the common tangent line. Here $n(k)$ is the number of clusters of size k, per unit volume. The slope of the tangent line is −2.05 in good agreement with theory. Panel b: Scaled cluster size distributions along with the theoretical form (solid line) expressed in eq 1.1 with $\lambda = -0.35$ and $\alpha = 1.35$. Here s is the average cluster size.

be the pth moment of the cluster size distribution and the mean cluster size $s = M_1/M_0$. For DLCA, the scaled cluster size distribution can be expressed as[16,20]

$$\Phi(x) = Ax^{-\lambda}e^{-\alpha x} \qquad (1.1)$$

for large values of x, where $\lambda = 1 - z^{-1}$, and $\alpha = p - \lambda$. In our simulations, $p = 1$ and if we consider $z = 0.74$, we find $\lambda = -0.35$, and $\alpha = 1.35$. Figure 5 shows that eq 1.1 with these values of λ and α fits the scaled cluster size distribution quite well for large values of x.

Conclusions

In summary, we have carried out a simulation study of selective aggregation in binary colloids with two different-sized particles. By varying the number fraction of the large to small particles, we have been able to reproduce the morphological characteristics of the clusters observed in experimental work of Hiddessen et al. The appearance of micelles, small clusters, and much larger branched structures depending on the number fraction of large to small particles follows almost exactly the same pattern as reported in the experiment. In addition, we have compared aggregation in binary colloids with the DLCA model by considering the fractal dimension, kinetic exponent, and cluster size distribution. The fractal dimension for the 2:1 number fraction starts out with a 2D DLCA value but crosses over to a larger value suggesting a DLCA to RLCA crossover in cluster morphology at late times. The kinetic exponent and the cluster size distribution, however, are consistent with 2D DLCA results. Further investigation of selective aggregation is certainly warranted, and a number of parameters are available to be adjusted in the search for a detailed understanding of this process. Those parameters include overall system volume fraction, size ratio of large to small particles, and number fraction. The determination of the conditions under which the system may enter a nonaggregating state is another alluring topic for further study. In addition, a fragmentation probability can also be imposed on the clusters which might lead to a steady-state *crystalline* morphology.

Acknowledgment. Financial support given by NASA under Grant Number NAG 3-2360 is gratefully acknowledged.

LA0356452

(20) Oh, C.; Sorensen, C. M. Light scattering study of fractal cluster aggregation near the free molecular regime. *J. Aerosol Sci.* **1997**, *28*, 937−957.